

Approach to the approximation of the transfer characteristic and correlation response of Fourier holography scheme

© A.V. Pavlov^{1,¶}, A.O. Gaugel¹, A.M. Alekseyev²

¹ ITMO University,
197101 St. Petersburg, Russia

² Laboratory Products Plant LLC „Freim“,
193230 St. Petersburg, Russia

¶ e-mail: avpavlov@itmo.ru

Received April 02, 2022

Revised May 05, 2022

Accepted June 09, 2022

An approach for approximating the transfer characteristic and response in the $+1$ th order of diffraction of a $4f$ Fourier holography scheme by a Gaussian-like model as applied to image processing with power-law spatial-frequency power spectra is proposed. The relations between the parameters of the approximation models and the reference image spectra are found by numerical simulation depending on the reference spectrum exponent. The approximation errors and the possibility of their optimization in the required range of spatial frequencies, determined by the nonlinearity of the exposure characteristics of holographic recording media, are shown. The validity of the approach is confirmed by comparing the results of numerical simulation with experimental data.

Keywords: holography, Fourier transform, spatial frequency spectrum, impulse response, recording media, exposure characteristic.

DOI: 10.21883/EOS.2022.09.54830.3478-22

Introduction

In optics, the approximation of linear systems is widely used, that allows to describe the structure of one of the two equal characteristics connected by the Fourier transform — its transfer function and/or impulse response [1]. Since it is not the complex-valued amplitudes which are directly measured, but the intensities of the wave fields, in practice, as applied to the classical $4f$ -Fourier holography scheme (Fig. 1), the transfer characteristic $H(\nu)$ is usually measured in the working order diffraction dependence of the local diffraction efficiency $\eta(\nu)$ (in terms of intensity) of the hologram on the spatial frequency ν

$$H^p(\nu) = \eta(\nu) = \hat{H}^p S(\nu), \quad (1)$$

where the superscript p indicates the diffraction order in which measurements are taken, $S(\nu)$ — the spatial-frequency power spectrum (Wiener spectrum) of the reference image used to record the hologram, and \hat{H} — operator of a holographic recording medium (HRM), taking into account the conditions for recording a hologram and the exposure characteristics of a HRS (EC HRS). Here we use the term transfer characteristic to distinguish (1) from a complex valued transfer function.

Instead of the impulse response, for practical reasons, the autocorrelation function (ACF) of the standard recorded on the hologram is often used, which is formed in the $+1$ -th order of diffraction in the output plane Out when the hologram is illuminated by the reference spectrum $S(\nu)$ (presenting a reference image in the input plane In) and

related to the transfer characteristic for the $+1$ th order of diffraction (1) by the Fourier transform

$$\mathcal{R}(\xi) = \hat{F}H^{+1}(\nu), \quad (2)$$

where ξ — coordinate in the back focal plane of the second Fourier transform lens L_2 — of the output plane of the circuit Out, \hat{F} — Fourier transform operator. The ACF is a diffraction-limited image of a point reference source used to record the hologram, i.e., the point blur function.

Here and below, where possible without compromising the meaning, we assume the separability of variables and use notations with functions of one variable to reduce the size of expressions. Consideration will be carried out in relation to the correlation response (2), i.e. to the $+1$ -th order of diffraction, which will be omitted below.

Real information is characterized by spacecountryreality-but-frequency power spectra, which in the article for brevity will be called simply spectra, with a power decay [2–4]. As applied to the Fourier holography scheme (Fig. 1), the transfer characteristic (1) with power-law spectra of reference images recorded on a hologram in a limited frequency range determined by the dynamic range of the EC HRS can often be approximated by exponential functions, since

a) frequency-contrast characteristics of information input paths, both optical and electronic, usually decrease with increasing frequency [1], i.e. information input paths play the role of additional low-frequency filters (LFF);

b) spatial limitation of the size of the processed information by the aperture of the frame window leads to a

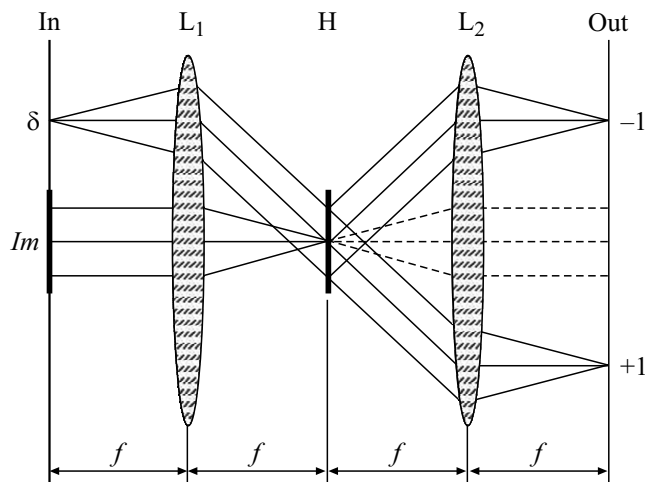


Figure 1. $4f$ -Fourier holography scheme with a flat off-axis reference beam: In and Out — input and output planes, respectively; L_1 , L_2 — Fourier transform lenses with focal lengths f , H — hologram, Im u δ — image and off-axis point reference source respectively, +1-th and -1-th — corresponding diffraction orders.

weakening of the zero and low-frequency components of the spectrum as a result of the convolution of the spectrum with the Fourier transform of the aperture — „low spatial“ frequencies;

c) EC HRS, represented by the dependence of the diffraction efficiency on exposure, usually have a sigmoidal form in the area of the direct (increasing) dependence [5–7], which causes additional bandpass filtering on the hologram — attenuation of the transfer characteristic (1) relative to the reference spectrum in the ranges of both low and high spatial frequencies [4,8–10];

d) additional filtering is also due to the form factor of the hologram [11], which is especially relevant for Fourier holograms and their special case — holographic matched filters, which in reality are matched only in a limited range spatial frequencies, determined both by the dynamic range of the EC HRS, and the conditions for recording the hologram — by choosing the frequency of equality of the local amplitudes of the spectrum and the plane reference beam [4,8–10]. In this case, the limited dynamic range of the EC HRS, which usually does not exceed two orders of magnitude, even in the case of a low-frequency hologram, as a rule, results, if not in a rejection, then in a very strong attenuation of zero and extremely low spatial frequencies.

From the point of view of clarity and convenience of the analytical description, the approximation of the transfer characteristics by Gaussian functions is attractive, but real spectra are characterized by an exponent of the argument (spatial frequency) different from 2, as a result of which the Gaussian model generally gives an inadequate description of the transfer characteristic and the ACF of the scheme. The use of other models makes it difficult to obtain compact and descriptive analytical expressions.

A number of papers are devoted to the search for a convenient and adequate model for approximating the response of the $4f$ -scheme; we mention [4,8–10] as applied to the correlation processing of images. In these studies, convenient and practically sufficient for the problem of recognition by the criterion of the magnitude of the signal-to-noise ratio [12] simplified approximation models were used. For example, in [8] the transfer characteristic (1) is approximated by a triangular Λ -function, and in the analytical description of the correlation response (2) only one parameter — its frequency (Λ -function) of the maximum, which in the first approximation corresponds to the frequency of equality of the local intensities of the spectrum of the reference image and the plane reference beam when recording the hologram. This approach turned out to be effective in the framework of the problem of recognizing images subjected to affine transformations relative to the reference ones.

But for a number of real recognition conditions, for example, in the presence of projective distortions of the recognizable image relative to the reference one, a simple and convenient model [8] turned out to be insufficient — a complete description of both spectra and holograms was required [13], which requires significant computational resources. The complication of problems solved by the Fourier holography method [14–22], including computer [16–19], and the corresponding complication of algorithms also actualizes the issue of adequate, visual and, which is important for practical real-time applications [16–19] of computationally inexpensive approximation.

This article shows the possibilities and limitations of approximating the transfer characteristic and correlation response of a Fourier holography scheme by a Gaussian-like model under the assumption that the hologram is recorded when the amplitude of the reference beam is equal to or exceeds the local amplitude of the reference beam at zero spatial frequency. The approach allows to find a compromise solution to the —visibility dilemma of the analytical model and to reduce the requirements for the processing power of the processor in the case of a computer implementation through the use of an analytical model.

1. Approach and approximation model

Let us represent the transfer characteristic of the circuit, i.e., the reference power spectrum $S(\nu)$ recorded on the hologram with a power decay, the exponential model

$$H(\nu) = \exp\left(-\ln(\alpha)\left(\frac{-\nu}{\nu_\alpha}\right)^D\right), \quad (3)$$

where ν — spatial frequency, $\eta(\nu)$ — dependence of the local diffraction efficiency of the hologram (DE) on the spatial frequency, D — exponent, ν_α — model parameter — frequency measured by level

$$\alpha = \frac{H(\nu_\alpha)}{H(0)} = \frac{\eta(\nu_\alpha)}{\eta(0)},$$

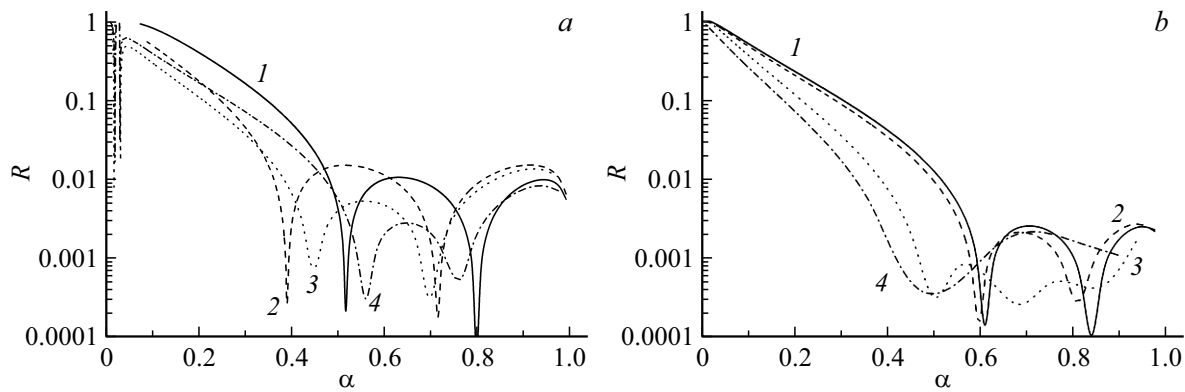


Figure 2. Dependences of the modulus of relative error R of approximation by the model (4) on the level of the spectrum α : 1 — the power spectrum of the power $S(v) = v^{-1.1}$ (a), $S(v) = v^{-2.6}$ (b), 2 — considering LFF; 3 — considering the sigmoidal EC HRS, FF and LFF ($a: D = 0.895, \nu_{0.606} = 11.6, b: D = 1.07, \nu_{0.606} = 6.57$); 4 — taking into account the sigmoidal EC HRS, FF and LFF ($a: D = 0.92, \nu_{0.606} = 11.8, b: D = 1.01, \nu_{0.606} = 5.551$).

i.e., defined as the ratio of the value of the transfer characteristic (local DE hologram) at a given frequency ν_α to its maximum value (within the — approach at zero frequency). The convenience of this model is that the parameter ν_α does not change when the exponent D changes, and for $\alpha = 0.606$ and $D = 2$ we have a Gaussian model. For simplicity and clarity, we will further consider a particular version of the level $\alpha = 0.606$, i.e.

$$H(v) = \exp\left(\frac{-v^D}{2\nu_{0.606}^D}\right), \quad (4)$$

where $\nu_{0.606}$ — parameter equal to the frequency at which the local diffraction efficiency of the hologram $\eta(v) = \exp(0.5) = 0.606$ from its maximum value $\eta(0)$.

The applicability and limitations of such an approximation are illustrated in Fig. 2, *a, b*, in which the absolute values of the relative errors of approximation by the model (4) of the transfer characteristics are given on a semilogarithmic scale, taking into account the factors mentioned in the introduction: low-frequency filtering (LFF), described by the Gaussian function, sigmoidal EC HRS(photographic plates „LOI2–653“, developer GP2 [23]) and form factor (FF), determined by the visibility of the spectrum interference pattern and flat reference beam. The errors are given for two power-law spectra: in Fig. 2, *a* — $S(v) = v^{-1.1}$ — satellite image of a winter landscape and fig. 2, *b* — $S(v) = v^{-2.6}$ — implementation of two-dimensional fractal Brownian motion adequately modeling the image cloud cover [24]. In the latter case, the spectral maximum at zero frequency, which stands out from the rest of the spectrum by 2.4 orders of magnitude, was attenuated during simulation, as was the case when recording real holograms due to the limited dynamic range of the EC HRS. The argument in Fig. 2 is the relative DE holograms

$$\alpha = \frac{H(\nu_\alpha)}{H(0)} = \frac{\eta(\nu_\alpha)}{\eta(0)},$$

t.e. Fig. 2 shows the relative error of approximation of the shape of the transfer characteristic scheme.

As can be seen from Fig. 2, with an increase in the exponent D , the approximation error decreases, and the selection of the parameters of the approximation model, which are physically determined by the mode of recording the hologram and its processing, including the EC HRS, makes it possible to optimize the relative error in the required range of spectrum intensities (local diffraction efficiency of the hologram $\eta(v)$ — transfer characteristic of the circuit) associated with the range of spatial frequencies. For the similar processing methods, a relative error of no more than 0.1 is traditionally considered acceptable, this level is exceeded only in the high-frequency region — the exponential model (4) gives underestimated values compared to the power law at high frequencies.

The correlation response of the holographic scheme in Fig. 1, as the Fourier transform of the function (4), is described by a similar expression only for $D = 2$, i.e. i.e. only for the Gauss function $G(v)$

$$\hat{F}G(v) = \hat{F} \exp\left(\frac{-v^2}{2\nu_{0.606}^2}\right) = \exp\left(\frac{-\xi^2}{2\gamma^2}\right), \quad (5)$$

where ξ — coordinate in the output (correlation) plane Out of the circuit in Fig. 1, $\gamma = \xi_{0.606} = \frac{1}{2\pi\nu_{0.606}}$ — parameter designation used in the article only for the parameter of the Fourier transform of the Gaussian function. If $D \neq 2$, then the Fourier transform of the function (4) when describing the response of the circuit, especially taking into account the additional filtering due to the EC HRS and the differences between the object (input) spectrum and the reference (recorded on the hologram) spectrum, gives a cumbersome and an inconvenient expression for practical purposes.

Let us take for the ACF, i.e., the Fourier transform of the function (4), also a Gaussian-like approximation model

$$\begin{aligned} \mathcal{R}(\xi) &= \hat{F}H^{+1}(\nu) = \hat{F} \exp\left(\frac{-\nu^D}{2\nu_{0.606}^D}\right) \\ &\approx \exp\left(\frac{-\xi^{d(D)}}{2(\xi_{0.606}(D, \nu_{0.606}))^{d(D)}}\right), \end{aligned} \quad (6)$$

where $d(D)$ — exponent depending on the exponent D in the spectrum model (4) and represent the parameter $\xi_{0.606}(D, \nu_{0.606})$ as follows way:

$$\xi_{0.606}(D, \nu_{0.606}) = Kp(D)\gamma, \quad (7)$$

where

$$Kp(D) = \frac{\xi_{0.606}(D, \nu_{0.606})}{\gamma} \quad (8)$$

— functional coefficient defining the relationship between the — parameter $\xi_{0.606}(D, \nu_{0.606})$ for an arbitrary exponent of — the argument D and the parameter γ of the Fourier transform of — the Gaussian function (5).

The exponent $d(D)$ can be represented in a similar way

$$d(D) = Kd(D)D, \quad (9)$$

where $Kd(D)$ — function coefficient.

Approximation (6), (7) is practically relevant due to the fact that the parameter $\xi_{0.606}(D, \nu_{0.606})$ characterizes the autocorrelation radius of the reference image recorded on the hologram $r = \sqrt{2}\xi(D, \nu_{0.606})$, i.e. determines the correlation estimate of the image information capacity — its generalized spatial frequency [4,12]

$$\Omega = \frac{L}{r} = \frac{L}{\sqrt{2}\xi_{0.606}(D, \nu_{0.606})},$$

where L — the size of the reference image when it is represented by a function of one argument. For a function of two coordinates, the generalized spatial frequency is defined as the ratio of the areas of the image and the correlation [12].

The question of validity of approximation (6) has a number of aspects, first of all:

1. The accuracy of the representation of the parameter $\xi_{0.606}(D, \nu_{0.606})$ by (7) — this question is relevant for the problems involving a single passage of radiation from the input plane of $4f$ -scheme of the Fourier holography (Fig. 1) to the output, in which the measurements are carried out: the intensity of the response or the radius of the correlation [12];

2. The accuracy of the impulse response approximation (or GM ACF) — this issue within our approach is reduced to the approximation of the exponent $d(D)$ by (9) and is relevant for more complex circuits, in which the impulse or correlation response is used for further processing, for example, resonant architecture circuits, including those implementing memory models [15,20,21] and nonmonotonic logic [22].

We will consider these questions in turn below. Since the representations (7) and (9) mathematically do not follow from (6), then the analytical finding of the functional coefficients $Kp(D)$ and $Kd(D)$ does not give convenient expressions. Therefore, the answers to these questions are found numerically.

2. Approximation of the correlation response

2.1. Approximation of the approximation response parameter

To find the functional coefficient $Kp(D)$ (8), which relates the parameters of the transfer function and the correlation response — of the global maximum of the autocorrelation function (GM ACF), a family of dependences of the ratio of the parameters $\xi_{0.606}/\gamma$ (6) for a series of values of the exponent D in the range $D \in [0.5, 4]$ and the range of values of the amplitude spectrum parameter (4) $\nu_{0.606} \in [1, 100]$ pixels for a spectrum realization length of $N = 2^{18} = 262144$. The values N and range of the spectrum parameter $\nu_{0.606}$ were chosen to ensure the accuracy of the numerical simulation of the correlation response.

Three approximation models were considered, previously selected for reasons of visual similarity of the graphical representation of the models with the calculated data: sigmoidal

$$Kp_s(D) = a_s(1 - \exp(-b_s(D - c_s)^{e_s})), \quad (10)$$

logarithmic (good visual match in the range $D \in [1.0, 2.0]$)

$$Kp_{ln}(D) = (\ln(D + a_{ln}))^{c_{ln}} + b_{ln} \quad (11)$$

and hyperbolic (good visual match in the range $D > 2.0$)

$$Kp_{hyp}(D) = 1.6\left(1 + \frac{1}{D}\right) + a_{hyp}, \quad (12)$$

where a, b, c and e — parameters, their letter indices point to the model. The selection of parameters was carried out according to the criterion of the minimum mean square deviation (RMS) of the value of the approximation of the results of numerical experiments. Table 1 shows the RMS values for these models depending on the approximation range.

As can be seen from the table, the narrowing of the approximation range leads to an increase in its accuracy, while the sigmoidal model (10) gives the best approximation for the criterion of RMS minimum RMS in wider ranges than models (11) and (12). Since the standard deviation is an estimate integral over the entire range, then Fig. 3, *a, b* shows the dependences of the relative approximation errors on the exponent D , allowing a more detailed idea of the approximation errors.

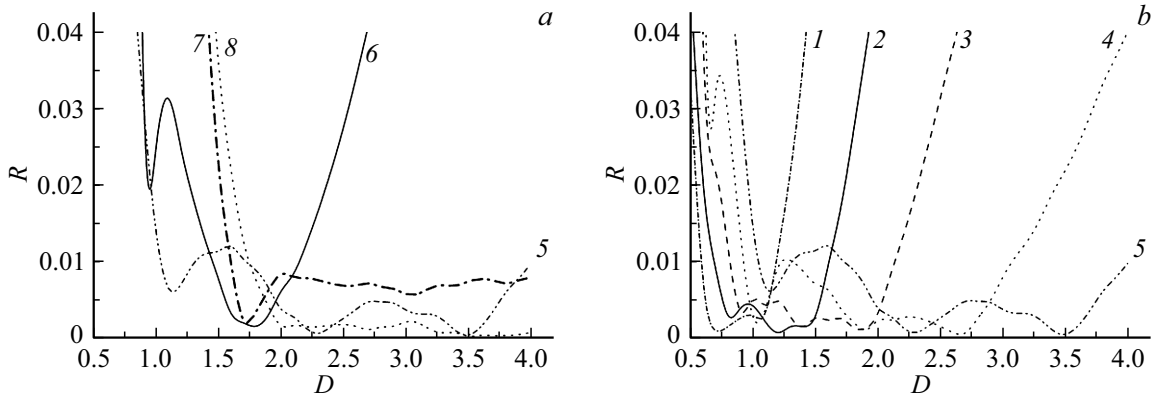


Figure 3. (a, b) Dependences of the relative error R of the approximation of the coefficient $Kp(D)$ on the exponent D : model (10) for the range $[0.5, 1.0]$ (1), $[0.5, 1.5]$ (2), $[0.5, 2.0]$ (3), $[0.5, 3.0]$ (4), $[0.5, 4.0]$ (5); model (11) for range $[1.0, 2.0]$ (6), model (12) for range $[2.0, 3.0]$ (7), $[3.0, 4.0]$ (8).

It can be seen that the model (10) gives a much more accurate approximation in both narrow and wide ranges. At the same time, we note that in the corresponding ranges, all models give an error that, on the whole, is more than an order of magnitude smaller than the threshold 0.1 traditionally accepted for analog calculations.

2.2. Approximation of the correlation response

The dependence $Kd(D)$ was found using the minimum standard deviation criterion of the approximation model (6) on the actual correlation response in the range $\xi \in [0, \xi_{max}]$, where ξ_{max} was determined by three criteria:

- a) representations of 99.5% of the spectrum energy as applied to $D = 2$ [1];
- b) dynamic range of measurement and, accordingly, approximation of the ACF 1st order;
- c) dynamic range of ACF measurement of the 2nd order.

The Kd dependences obtained in numerical experiments were approximated by the model

$$Kd(D) = A - B_1 \left(1 - \exp\left(\frac{-D}{C_1}\right) \right) - B_2 \left(1 - \exp\left(\frac{-D}{C_2}\right) \right), \tag{13}$$

where A, B_1, B_2, C_1 and C_2 — parameters: values and RMS of approximation for each of these options are given in Table 2.

Figure 4 shows on a semi-logarithmic scale the relative errors of approximation of the GM ACF form for the variant a), where $\beta = \frac{\mathcal{R}(\xi)}{\mathcal{R}(0)}$ — relative amplitude of GM ACF. For b) and c), the dependences had a similar form, but with the expansion of the approximation range, the relative approximation error generally increased.

3. Experimental procedure

To experimentally confirm the validity of the above approach, in the scheme of Fig. 1, a series of Fourier

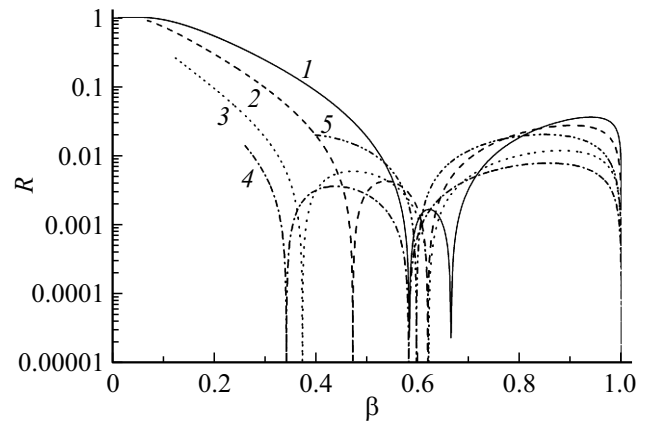


Figure 4. Relative errors in the approximation of the GM ACF shape when choosing the approximation range from the condition of representing 99.5% of the spectrum energy as applied to $D = 2$: $D = 0.5$ (1), 1.0 (2), 1.5 (3), 2.5 (4), 4.0 (5).

holograms of the image of two-dimensional fractal Brownian motion (DFBM) was recorded, the spectrum of which is described by the model [23]

$$S(\nu) = \nu^{2\mathcal{H}+1},$$

where $\mathcal{H} \in [0, 1]$ — Hurst parameter. As a standard for recording holograms, we used the DFBD implementation shown in Fig. 5 with the value of the Hurst parameter $\mathcal{H} = 0.8$, which corresponds to the exponent of the power spectrum $D = 2.6$. The holograms were recorded at different ratios of the amplitudes of the signal and reference beams, i.e. they had different form factors and were matched in different ranges of spatial frequencies. Recorded holograms were presented with both reference and low-frequency Gaussian filtered images with different values of the filter parameter. Correlation responses were measured using LI-602 dissector characterized by a wide dynamic range.

Table 1. RMS and values of approximation parameters $K_p(D)$ for different ranges D

Range D	Model (10)		Model (11) $a_{ln} = 0.2, b_{ln} = 0.2$		Model (12)	
	parameters	RMS	parameter c_{ln}	RMS	parameter a_{hyp}	RMS
[0.5,4.0]	$a_s = 1.44712$ $b_s = 0.74342$ $c_s = 0.46575$ $e_s = 1.18905$	0.0076	0.85	0.081	0.2	0.328
[1,4.0]			0.85	0.0765	0.21	0.047
[1,3.5]			0.85	0.053	0.21	0.051
[0.5,3.0]	$a_s = 1.37323$ $b_s = 0.7904$ $c_s = 0.4385$ $e_s = 1.29348$	0.0052				
[1,3.0]			0.9	0.032	0.21	0.057
[1,2.5]			0.9	0.014	0.21	0.066
[0.5,2.0]	$a_s = 1.222$ $b_s = 0.889$ $c_s = 0.393$ $e_s = 1.48578$	0.00286				
[1,2.0]			0.9	0.005	0.21	0.08
[0.5,1.5]	$a_s = 1.056$ $b_s = 1.0073$ $c_s = 0.35825$ $e_s = 1.6775$	0.00161				
[0.5,1.0]	$a_s = 0.8592$ $b_s = 1.17409$ $c_s = 0.33101$ $e_s = 1.87929$	0.00095				
[2.0,4.0]	$a_s = 1.619$ $b_s = 1.00332$ $c_s = 0.63857$ $e_s = 1.05991$	0.0006				
[3.0,4.0]	$a_s = 1.615$ $b_s = 0.67154$ $c_s = 0.44753$ $e_s = 0.80415$	0.00046	0.6	0.012	0.2	0.002
[2.0,3.0]	$a_s = 1.619$ $b_s = 1.00332$ $c_s = 0.63857$ $e_s = 1.05991$	0.00049	0.7	0.005	0.2	0.003

Fig. 6 shows three examples of the responses of the circuit in Fig. 1: (1) and (2) — responses to the reference image Fig. 5 of two holograms from the series, which can be defined as high-frequency (1) and low-frequency (2), measured values of the GM ACF parameter $\xi_{0.606} = 0.175$ mm and $\xi_{0.606} = 0.94$ mm, respectively, and also (3) — the response of a high-frequency hologram to an image subjected to low-pass

filtering by a Gaussian filter, the measured value of the response parameter $\xi_{0.606} = 0.5$ mm, correlation coefficient — 0.128. The experimentally measured responses (points) were approximated by the model (6) (lines).

Fig. 6 shows a good agreement between the Gaussian-like model (6) of the approximation of the correlation response (GM ACF) and the experimental data when both reference

Table 2. Approximation model parameter values (13) and RMS

Range selection option	Parameter values					RMS of approximation
	A	B_1	B_2	C_1	C_2	
A)	4.79749	2.59236	1.8393	0.25871	1.8771	0.0027
b)	5.91143	4.4454	1.85496	0.43043	6.26752	0.02196
c)	8.92392	7.5411	64.29551	0.20088	313.6806	0.00976

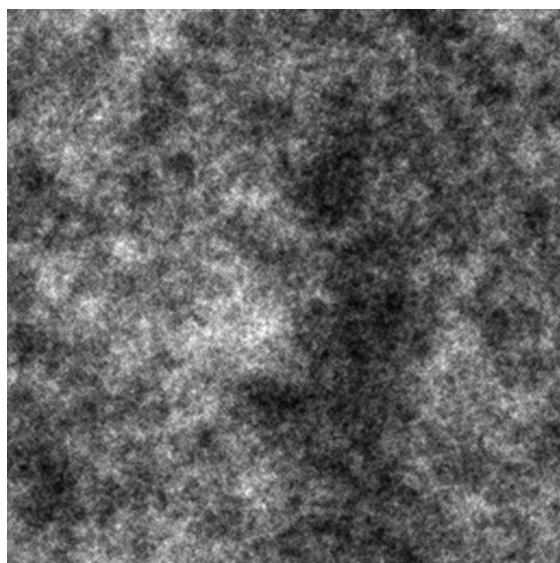


Figure 5. Implementation of two-dimensional fractal Brownian motion with Hurst parameter $\mathcal{H} = 0.8$.

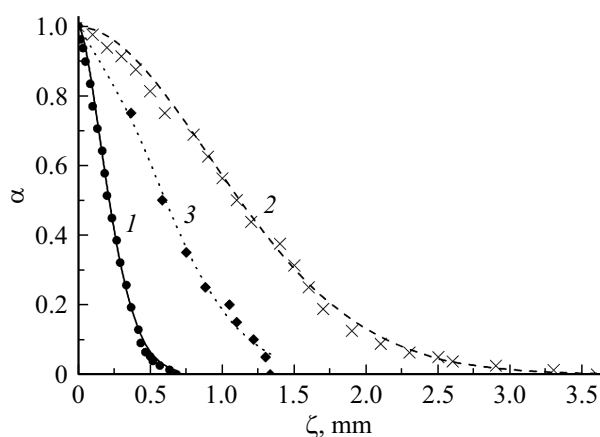


Figure 6. Global maxima of autocorrelation functions: 1 — high-frequency hologram; 2 — low-frequency hologram; 3 — response of a high-frequency hologram to a standard subjected to LFF; dots — experiment, lines — approximation (6); RMS of approximation: 1 — $4.35 \cdot 10^{-4}$, 2 — $5.36 \cdot 10^{-4}$, 3 — $7.214 \cdot 10^{-4}$ (3).

(curves 1 and 2) and smeared low-frequency image filter (curve 3).

Conclusion

Thus, when the Fourier holography scheme processes information with power-law spectra, due to the limited dynamic range of holographic recording media, the transfer characteristic and autocorrelation function can be approximated with an accuracy acceptable for practical purposes by a Gaussian-like model. The exponential models of the spectra are characterized by a significant decrease in the proportion of high-frequency components compared to the exponential ones, but in practice this factor is largely leveled out both by low-frequency filtering in the information input paths and by the nonlinearity of the exposure characteristics of holographic recording media, which leads to a limited frequency range of the transfer characteristic. In some cases, the limitation of the frequency range is already necessary from the conditions of the problem, for example, to ensure the required signal-to-noise ratio in the correlation comparison of images [12]. The selection of the parameters of the approximation model allows you to optimize the model for the required frequency range.

In a number of practical problems, to input computer-synthesized holographic filters into the processor, space-time light modulators with a pronounced discrete structure and a limited number of quantization levels are used [18,19]. In this case, the described approach allows to optimize the requirements for computing power and memory size for calculating the filter.

Information on authors contribution

The contribution of A.V. Pavlov is in the formulation of the problem, the formation of an approach, the development of software, the planning and implementation of numerical and natural experiments, the processing of their results, writing the article, the contribution of A.O. Gaugel consists in the participation in numerical simulation, the contribution of A.M. Alekseyev — in participation in full-scale experiments.

Conflict of interest

The authors declare that they have no conflict of interest.

References

- [1] M.M. Miroshnikov. *Teoreticheskie osnovy optiko-elektronnyh priborov*. (Mashinostroenie, Leningrad, 1977) 600 p. (in Russian).
- [2] A.M. Yaglom. *Korrelyacionnaya teoriya stacionarnykh sluchajnykh funktsij*. (Gidrometeoizdat, Leningrad, 1981) 280 p.
- [3] A.E. Altynov, V.V. Gruzinov, I.V. Mishin. *Izv. vuzov. Geodeziya i aerofotosyomka*, (1), 34 (2017).
- [4] A.M. Kuleshov, E.I. Shubnikov, S.A. Smaeva. *Opt. Spectrosc.*, **60** (6), 791 (1986).
- [5] V.A. Barachevsky. *Opt. Spectrosc.*, **124** (3), 373 (2018). DOI: 10.21883/OS.2018.03.45659.238-17
- [6] L.P. Amosova, N.I. Pletneva, A.N. Chaika, J. *Optical Technology*, **72** (6), 469 (2005). DOI: 10.1364/JOT.72.000469
- [7] L.P. Amosova, A.N. Chaika, *Technical Physics Lett.*, **33** (6), 255 (2007). DOI: 10.1134/S1063785007030200
- [8] E.I. Shubnikov, A.M. Kuleshov. *Opt. Spectrosc.*, **55** (1), 94 (1983).
- [9] A.M. Kuleshov, E.I. Shubnikov. *Opt. Spectrosc.*, **60** (3), 369 (1986).
- [10] S.A. Aleksandrina, A.M. Kuleshov. *Opt. i spectr.*, **68** (3), 652 (1990).
- [11] S.A. Shoydin, M.S. Kovalev. *Opt. Spectrosc.*, **128** (7), 885 (2020). DOI: 10.21883/OS.2020.07.49557.108-20
- [12] E.I. Shubnikov. *Opt. Spectrosc.*, **62** (2), 268 (1987).
- [13] A.V. Pavlov. *Opt. Spectrosc.*, **78** (1), 135 (1995).
- [14] V.V. Orlov. *Quantum Electronics*, **47** (8), 773 (2017) DOI: 10.1070/QEL16337
- [15] A.V. Pavlov, V.V. Orlov. *Quantum Electronics*, **49** (3), 246 (2019). DOI: 10.1070/QEL16748
- [16] P.A. Ruchka, N. M. Verenikina, I.V. Gritsenko, E.Yu. Zlokazov, M.S. Kovalev, G.K. Krasin, S.B. Odinkov, N.G. Stsepuro. *Opt. Spectrosc.*, **127**, 618 (2019). DOI: 10.21883/OS.2019.10.48358.172-19
- [17] M.S. Kovalev, G.K. Krasin, S.B. Odinkov, A.B. Solomashenko, E.Yu. Zlokazov. *Optics Express*, **27** (2), 1563 (2019). DOI: 10.1364/OE.27.001563
- [18] E.Yu. Zlokazov. *Quantum Electronics*, **50** (7), 643 (2020). DOI: 10.1070/QEL17291
- [19] N.N. Evtikhiev, E.Yu. Zlokazov, V.V. Krasnov, V.G. Rodin, R.S. Starikov, P.A. Cheremkhin. *Quantum Electronics*, **50** (7), 667 (2020). DOI: 10.1070/QEL17295
- [20] S. Rothe, P. Daferner, S. Heide, D. Krause, F. Schmieder, N. Koukourakis, J.W. Czarske. *Optics Express*, **29** (23), 37602 (2021). DOI: 10.1364/OE.434842
- [21] H.J. Mager, O. Wess, W. Waidelich. *Opt. Commun.*, **9** (2), 156 (1973). DOI: 10.1016/0030-4018(73)90248-4
- [22] A.V. Pavlov. *Kompyuternaya optika*, **44** (5), 728 (2020). DOI: 10.18287/2412-6179-CO-668
- [23] I.R. Ptotas, V.I. Mikhailove, Yu.A. Krakau, G.M. Shepetukha, I.V. Baranovs, Yu.E. Usanoc, L.V. Matsiyevich, E.I. Mikhailova. *Materialy SHestoj vsesoyuznoj shkoly po golografii*. Yerevan, February 11–17, 1974. P. 529–531. URL: <http://bsfp.media-security.ru/school6/31.htm>
- [24] Richard M. Crownover. *Introduction to Chaos and Fractals*. (Jones and Bartlett Publishers, Inc., Boston, London, 1995).